Hindawi Publishing Corporation
Advances in Condensed Matter Physics
Volume 2013, Article ID 920369, 6 pages
http://dx.doi.org/10.1155/2013/920369

Research Article

Synthesis, Tunable Multicolor Output, and High Pure Red Upconversion Emission of Lanthanide-Doped Lu_2O_3 Nanosheets

Lingzhen Yin, Tianmei Zeng, Zhigao Yi, Chao Qian, and Hongrong Liu

College of Physics and Information Science and Key Laboratory of Low-Dimensional Quantum Structures and Quantum Control of the Ministry of Education, Hunan Normal University, Changsha, Hunan 410081, China

Correspondence should be addressed to Hongrong Liu; hrliu@hunnu.edu.cn

Received 9 October 2013; Accepted 22 November 2013

Academic Editor: Jianhua Hao

Yb^{3+} and Ln^{3+} (Ln = Er, Ho) codoped Lu_2O_3 square nanocubic sheets were successfully synthesized via a facile hydrothermal method followed by a subsequent dehydration process. The crystal phase, morphology, and composition of hydroxide precursors and target oxides were characterized by X-ray diffraction (XRD), field emission scanning electron microscope (FE-SEM), and energy-dispersive X-ray spectroscope (EDS). Results present the as-prepared Lu_2O_3 crystallized in cubic phase, and the monodispersed square nanosheets were maintained both in hydroxide and oxides. Moreover, under 980 nm laser diode (LD) excitation, multicolor output from red to yellow was realized by codoped different lanthanide ions in Lu_2O_3. It is noteworthy that high pure strong red upconversion emission with red to green ratio of 443.3 of Er-containing nanocrystals was obtained, which is beneficial for *in vivo* optical bioimaging.

1. Introduction

In the past few decades, lanthanide-doped upconversion phosphors have received considerable attention due to their application in display systems [1], optical processing sensors [2], solid-state lasers [3], fluorescent detection, and label of biomolecules [4]. More importantly, as the applications in biological assays and medical imaging, the conventional semiconductor quantum dots were limited due to cytotoxicity, photobleaching, photodamage and low signal-to-noise ratio for excitation with short wavelength (usually ultraviolet and visible light) [5, 6]. Upconversion nanocrystals (UCNCs), which overcome those problems and absorb long wavelength (usually near infrared (NIR) light) and emit short wavelength, were believed to be a new kind of fluorescence materials [7, 8]. Besides, UCNCs have low radiation damage, chemical stability, and deep penetration of NIR excitation source compared with conventional fluorescent materials [9, 10].

It is well known that the luminescence property of UCNCs is affected by a combination of different host/activator, doping concentrations, nanocrystal size, shape, and the coatings [11–13]. Therefore, it is important to select appropriate host matrixes for achieving excellent luminescence property. Lutetium oxides are one of the excellent host matrix for ionizing radiation detection and X-ray phosphors because of their unique properties: high atomic number of Lu (71) and high density (9.42 g/cm^{-3}) [14, 15]. Besides, the ionic radius of Lu^{3+} (1.117 Å) is closer to the radius of Yb^{3+} (1.125 Å) than that of other lanthanide ions [16], which may improve the stability of UCNCs while doping high concentration Yb^{3+}. More importantly, the energy levels of Lu, especially the 4f orbital, make Lu-containing structure of stronger luminescence intensity than Y-containing crystal [17–19], which was known as very efficient phosphors.

As a potential host matrix, lutetium oxides have received many research interests. Studies on the synthesis of Lu_2O_3 with controlled size and various morphologies have been extensively carried out [20–22]. In addition, the luminescence properties of Lu-containing nanocrystals, for example, multicolor output manipulation by changing the reaction temperature, doping different lanthanide ions, and tuning the concentration of sensitizer or activator ions, have been widely investigated [23–25]. However, most of those researches are about lutetium fluorides, and the study on lanthanide ions-doped Lu_2O_3 was still limited. Furthermore, the lutetium oxide nanocubic sheets have rarely been mentioned.

Herein, we have prepared Yb^{3+}, Ln^{3+} (Ln = Er, Ho) codoped Lu_2O_3 via a simple and green hydrothermal method followed by a dehydration process [26]. Moreover, under the excitation of 980 nm laser diode, strong eye-visible red and yellow lights were observed. And the mechanism of the pure red upconversion emission was discussed in detail.

2. Experimental Section

Rare earth nitrates $RE(NO_3)_3{\cdot}6H_2O$ (RE = Lu, Yb, Er, Ho, 99.99%) were purchased from Sinopharm Chemical Reagent Co., Ltd (China). All other materials are of analytical grade and used directly without further purification.

2.1. Sample Preparation. Yb^{3+} and Ln^{3+} (Ln = Er, Ho) codoped Lu_2O_3 with a composition of $Lu_{1.60-x}Yb_{0.40}Ln_xO_3$ ($x = 0.04$) was prepared by using a facile hydrothermal method followed by a dehydration process [26]. As for the synthesis of Lu_2O_3:Yb^{3+}, Er^{3+}, the corresponding amount of rare earth nitrate (total amount: 1 mmol) was thoroughly mixed with 20 mL distilled water, then NaOH solution with $[OH^-] = 5$ mol/L was gradually added to obtain the hydroxide precipitates and adjust the pH to 14 under strong stirring. After being stirred 10 mins, the mixed solution was transferred into autoclaves to carry out a hydrothermal treatment at 180°C for about 12 h, and after cooling down to room temperature the hydroxide precursor was purified by centrifugation, washed with distilled water several times, and then dried at 80°C. At last, the corresponding rare earth-doped oxides were prepared successfully through the subsequent dehydration at 800°C for about 4 hours. The Yb/Ho codoped Lu_2O_3 was prepared in a similar procedure.

2.2. Characterization. Power X-ray diffraction (XRD) patterns of the samples were measured with D/max 2500/PC diffractometer using Cu-Kα radiation ($\lambda = 1.5406$ Å) at 40 kV and 250 mA. The morphology and composition of the samples were recorded on a FE-SEM equipped by an EDS system (FEI NanoSEM 450). The upconversion spectra were recorded using R-500 spectrophotometer under an unfocused 980 nm LD excitation at room temperature, and the corresponding digital photographs were taken by a digital camera under 980 nm infrared irradiation.

3. Results and Discussion

3.1. Phase and Morphology. Figure 1 shows the XRD patterns of Lu_2O_3:Yb^{3+}, Ho^{3+} and the standard cubic phase Lu_2O_3 (JCPDS no. 86-2475) for comparison. As demonstrated, all diffraction peaks of Yb-Ho codoped Lu_2O_3 are perfectly indexed to the pure cubic phase Lu_2O_3 and no other impurity peaks are detected, implying the high purity cubic phase structure is obtained via the facile hydrothermal approach. Moreover, compared with the standard diffraction peaks, there are very little deviations because the radius of main doped ion Yb^{3+} (1.125 Å) is very close to that of Lu^{3+} (1.117 Å) [16].

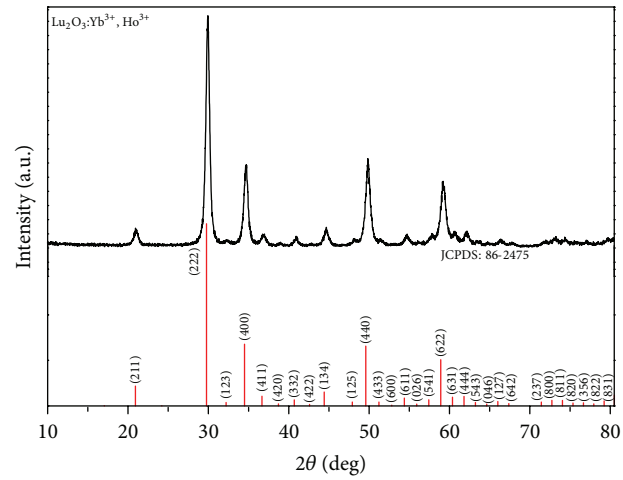

FIGURE 1: XRD patterns of Yb^{3+} and Ho^{3+} codoped Lu_2O_3 powder obtained via a hydrothermal approach (black line); the red lines indicate the standard data of pure cubic Lu_2O_3 structure (JCPDS: 86-2475).

More information about morphology and composition can be obtained by FE-SEM observation and EDS analysis. Figure 2 shows the FE-SEM images of precursor $Lu(OH)_3$ (Figures 2(a) and 2(b)) and Lu_2O_3:Yb^{3+}, Ho^{3+} (Figures 2(c) and 2(d)). As shown in FE-SEM images, all of these two samples present square nanosheets structure and no obvious difference between the two samples in the morphology is founded, implying the samples have well thermal stability. The corresponding EDS (Figure 2(e)) shows the main elements components are Lu, O, Yb, and Ho, implying the Yb and Ho ions are doped into the host matrix successfully.

3.2. Upconversion Luminescent Properties. Figure 3(a) demonstrates the upconversion luminescence spectra of Yb-Er codoped Lu_2O_3 nanocrystals. Under the excitation of 980 nm laser diode, an intense red emission band centered at 655 nm and a very weaker green emission area are observed. After magnifying 350 times (left inset in Figure 3(a)), the green emission area includes two weak bands centered at 526 nm and 542 nm, respectively. Moreover, the red to green (R/G) ratio is measured to a very large value of 443.3, resulting in a pure red upconversion emission, which is also verified by the digital photograph (right inset of Figure 3(a)) and CIE chromaticity coordinates ($X = 0.6312$, $Y = 0.33346$) illustrated in Figure 3(b). When codoped Yb-Ho ions to Lu_2O_3 nanocrystals, the as-prepared structure has both intense green and red emissions (Figure 3(c)). Therefore, bright eye-visible yellow light was observed (inset of Figures 3(c) and 3(d)), differing from the red light seen from the Yb-Er codoped samples. Therefore, the multicolor tuning from red to yellow can be achieved by simply doping different activator ions such as Er^{3+} and Ho^{3+}. More importantly, the pure red upconversion emission with large R/G ratio of 443.3 was realized, which is more beneficial for optical bioimaging for deep tissue penetration.

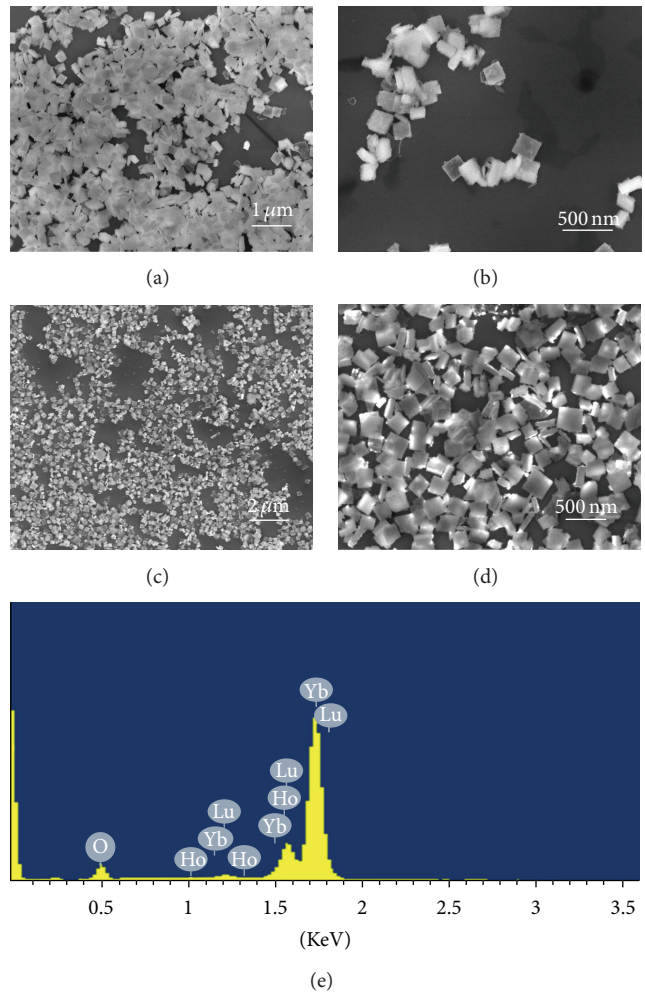

FIGURE 2: FE-SEM images of the as-prepared precursor $Lu(OH)_3$:Yb^{3+}, Ho^{3+}: (a) low magnification, (b) high magnification and obtained FE-SEM images of target Lu_2O_3:Yb^{3+}, Ho^{3+}, (c) low magnification, (d) high magnification, and (e) EDS of the obtained Lu_2O_3:Yb^{3+}, Ho^{3+} nanocubic sheets.

To reveal the possible upconversion mechanism, a simplified energy level diagram with indicated pathways is presented (Figure 4). As shown, the two weak green emissions of Yb-Er co-doped samples are assigned to the $^2H_{11/2} \rightarrow {}^4I_{15/2}$ (526 nm) and $^4S_{3/2} \rightarrow {}^4I_{15/2}$ (542 nm) transitions of Er^{3+}, and the red emission is attributed to the $^4F_{9/2} \rightarrow {}^4I_{15/2}$ transition of Er^{3+}. The high intensity ratio of the red to green emission can be explained from Figure 4. One reason of the red emission enhancement is that energy transfer from sensitizer ion Yb^{3+} at $^2F_{5/2}$ state to activator ion Er^{3+} through $^4I_{15/2} \rightarrow {}^4I_{11/2}$ transition, and then perform a nonradiative decay, which increase the number of Er^{3+} at $^4I_{13/2}$ level, at last, energy transfer from Yb^{3+} at $^2F_{5/2}$ state to Er^{3+} through $^4I_{13/2} \rightarrow {}^2F_{9/2}$. Another reason is the efficient cross-relaxation (CR) process of Er^{3+}: $^4I_{11/2} + {}^4F_{7/2} \rightarrow {}^4F_{9/2} + {}^4F_{9/2}$ illustrated in Figure 4. The CR process strengthens the red band and weakens the green emission because most of the ions at $^4F_{7/2}$ state transfer to $^4F_{9/2}$ directly bypassing the $^2H_{11/2}$ and $^4S_{3/2}$, which contribute to the green emission [23–25].

On the other hand, the green and red upconversion emissions of Ho containing sample are mainly attributed to the transitions $^5F_4 \rightarrow {}^5I_8$ (541 nm), $^5S_2 \rightarrow {}^5I_8$ (551 nm), $^5F_5 \rightarrow {}^5I_8$ (640–678 nm) of Ho^{3+} (Figure 4). As illustrated in Figure 4, all the processes need two-photo energy transfer; the red emission state $^5F_5$ is attributed to phonon-assisted energy transfer: $^5I_7(Ho^{3+}) \rightarrow {}^5F_5(Ho^{3+})$ and non-radiative decay from $^5S_2$. When doping high concentration Yb^{3+} (20%), all the three emissions are enhanced and lead to an intense eye-visible yellow light with CIE chromaticity coordinates at $X = 0.419$, $Y = 0.5318$.

4. Conclusion

In summary, monodispersed Lu_2O_3 co-doped with Yb^{3+} and Ln^{3+} (Ln = Er, Ho) square nanocubic sheets were successfully fabricated with a simple hydrothermal method.

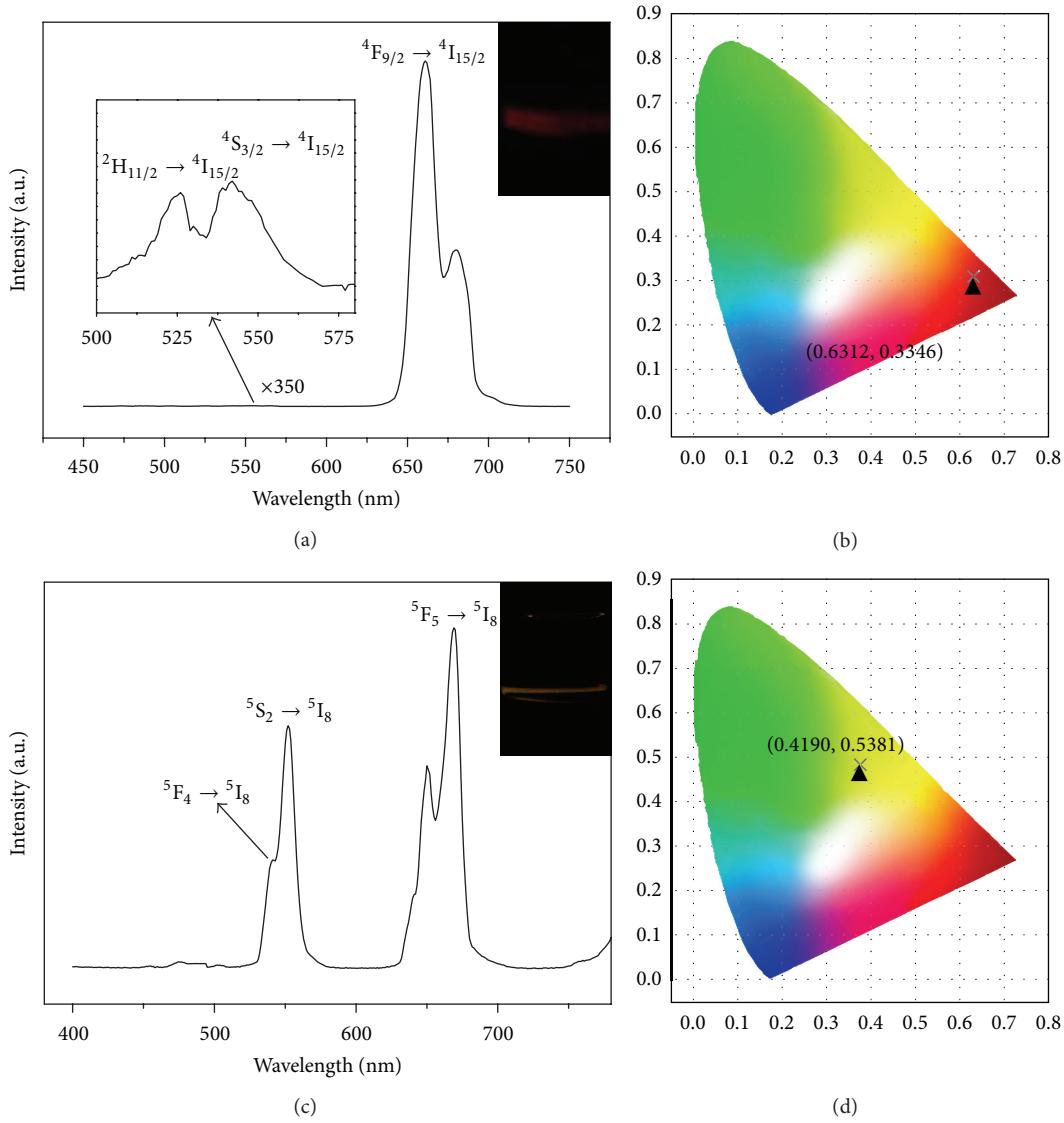

Figure 3: (a) UC spectra of Lu_2O_3:Yb/Er, (b) CIE chromaticity coordinates diagram of Lu_2O_3:Yb/Er, (c) UC spectra of Lu_2O_3:Yb/Ho, and (d) CIE chromaticity coordinates diagram of Lu_2O_3:Yb/Ho; the right insets of (a) and (c) are the corresponding digital photographs of 1 wt% water soluble of the samples.

The upconverted luminescence properties of as-prepared samples were well investigated under excitation of 980 nm laser diode. By changing the doped ions from Er to Ho, the upconversion emissions transform from eye-visible red to bright yellow light. Moreover, high pure red upconversion emission was obtained in Yb/Er codoped sample, which is suitable for high contrast optical bioimaging with absence of autofluorescence owing to the low tissue absorption at red light area (655 nm).

Acknowledgments

This work was supported by the National Natural Science Foundation of China (no. 51102202), New Century Excellent Talents in University (NCET-13-0787), Specialized Research Fund for the Doctoral Program of Higher Education of China (no. 20114301120006) and Hunan Provincial Natural Science Foundation of China (nos. 12JJ4056 and 13JJ1017), the Scientific Foundation of Ministry of Education (212119), and Scientific Research Fund of Hunan Provincial Education Department (13B062).

References

[1] E. Downing, L. Hesselink, J. Ralston, and R. Macfarlane, "A three-color, solid-state, three-dimensional display," *Science*, vol. 273, no. 5279, pp. 1185–1189, 1996.

[2] B. M. van der Ende, L. Aarts, and A. Meijerink, "Lanthanide ions as spectral converters for solar cells," *Physical Chemistry*

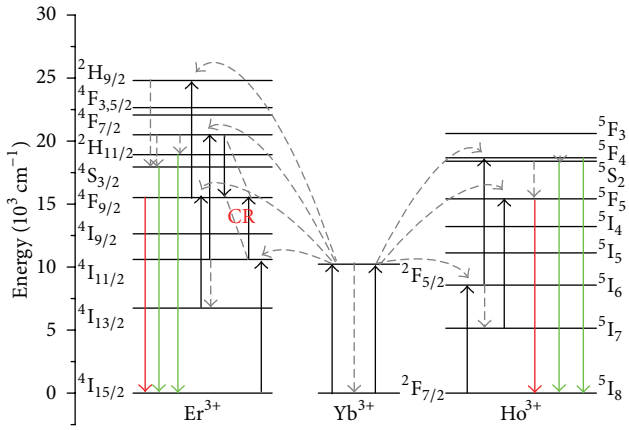

FIGURE 4: Schematic energy level diagrams of Yb^{3+}, Er^{3+}, and Ho^{3+} ions and proposed upconversion mechanism.

Chemical Physics, vol. 11, no. 47, pp. 11081–11095, 2009.

[3] G. F. Wang, Q. Peng, and Y. D. Li, "Lanthanide-doped nanocrystals: synthesis, optical-magnetic properties, and applications," *Accounts of Chemical Research*, vol. 44, no. 5, pp. 322–332, 2011.

[4] H. R. Liu, W. Lu, H. B. Wang et al., "Simultaneous synthesis and amine-functionalization of single-phase $BaYF_5$:Yb/Er nanoprobe for dual-modal *in vivo* upconversion fluorescence and long-lasting X-ray computed tomography imaging," *Nanoscale*, vol. 5, no. 13, pp. 6023–6029, 2013.

[5] N. Lewinski, V. Colvin, and R. Drezek, "Cytotoxicity of nanopartides," *Small*, vol. 4, no. 1, pp. 26–49, 2008.

[6] J. M. Klostranec and W. C. W. Chan, "Quantum dots in biological and biomedical research: recent progress and present challenges," *Advanced Materials*, vol. 18, no. 15, pp. 1953–1964, 2006.

[7] S. J. Zeng, M. K. Tsang, C. F. Chan, K. L. Wong, and J. H. Hao, "PEG modified $BaGdF_5$:Yb/Er nanoprobes for multi-modal upconversion fluorescent, *in vivo* X-ray computed tomography and biomagnetic imaging," *Biomaterials*, vol. 33, no. 36, pp. 9232–9238, 2012.

[8] F. Auzel, "Upconversion and anti-stokes processes with f and d ions in solids," *Chemical Reviews*, vol. 104, no. 1, pp. 139–174, 2004.

[9] S. J. Zeng, J. J. Xiao, Q. B. Yang, and J. H. Hao, "Bi-functional $NaLuF_4$:Gd^{3+}/Yb^{3+}/Tm^{3+} nanocrystals: structure controlled synthesis, near-infrared upconversion emission and tunable magnetic properties," *Journal of Materials Chemistry*, vol. 22, no. 19, pp. 9870–9874, 2012.

[10] J. C. Boyer, F. Vetrone, L. A. Cuccia, and J. A. Capobianco, "Synthesis of colloidal upconverting $NaYF_4$ nanocrystals doped with Er^{3+}, Yb^{3+} and Tm^{3+}, Yb^{3+} via thermal decomposition of lanthanide trifluoroacetate precursors," *Journal of the American Chemical Society*, vol. 128, no. 23, pp. 7444–7445, 2006.

[11] G. Z. Ren, S. J. Zeng, and J. H. Hao, "Tunable multicolor upconversion emissions and paramagnetic property of monodispersed bifunctional lanthanide-doped $NaGdF_4$ nanorods," *Journal of Physical Chemistry C*, vol. 115, no. 41, pp. 20141–20147, 2011.

[12] F. Wang and X. G. Liu, "Recent advances in the chemistry of lanthanide-doped upconversion nanocrystals," *Chemical Society Reviews*, vol. 38, no. 4, pp. 976–989, 2009.

[13] S. J. Zeng, G. Z. Ren, C. F. Xu, and Q. B. Yang, "Modifying crystal phase, shape, size, optical and magnetic properties of monodispersed multifunctional $NaYbF_4$ nanocrystals through lanthanide doping," *CrystEngComm*, vol. 13, no. 12, pp. 4276–4281, 2011.

[14] J. Trojan-Piegza, E. Zych, D. Hreniak, W. Stręk, and L. Kępiński, "Structural and spectroscopic characterization of Lu_2O_3:Eu nanocrystalline spherical particles," *Journal of Physics Condensed Matter*, vol. 16, no. 39, pp. 6983–6994, 2004.

[15] J. C. Boyer, F. Vetrone, J. A. Capobianco, A. Speghini, and M. Bettinelli, "Variation of fluorescence lifetimes and judd-ofelt parameters between Eu^{3+} doped bulk and nanocrystalline cubic Lu_2O_3," *Journal of Physical Chemistry B*, vol. 108, no. 52, pp. 20137–20143, 2004.

[16] R. D. Shannon, "Revised effective ionic radii and systematic studies of interatomic distances in halides and chalcogenides," *Acta Crystallographica A*, vol. 32, no. 5, pp. 751–767, 1976.

[17] P. Rambaldi, R. Moncorgé, J. P. Wolf, C. Pédrini, and J. Y. Gesland, "Efficient and stable pulsed laser operation of Ce:$LiLuF_4$ around 308 nm," *Optics Communications*, vol. 146, no. 1–6, pp. 163–166, 1998.

[18] V. Sudesh and K. Asai, "Spectroscopic and diode-pumped-laser properties of Tm,Ho:YLF; Tm,Ho:LuLF; and Tm,Ho:LuAG crystals: a comparative study," *Journal of the Optical Society of America B*, vol. 20, no. 9, pp. 1829–1837, 2003.

[19] C. Maunier, J. L. Doualan, R. Moncorgé, A. Speghini, M. Bettinelli, and E. Cavalli, "Growth, spectroscopic characterization, and laser performance of Nd:$LuVO_4$, a new infrared laser material that is suitable for diode pumping," *Journal of the Optical Society of America B*, vol. 19, no. 8, pp. 1794–1800, 2002.

[20] H. J. Qiu, Y. Shi, J. J. Xie, J. Xie, L. L. Zhang, and F. F. Xu, "Hydrothermal route to Eu doped LuO(OH) and Lu_2O_3 nanorods," *Science China Technological Sciences*, vol. 53, no. 6, pp. 1576–1582, 2010.

[21] H. Guo, M. Yin, N. Dong, M. Xu, L. R. Lou, and W. P. Zhang, "Effect of heat-treatment temperature on the luminescent properties of Lu_2O_3:Eu film prepared by Pechini sol-gel method," *Applied Surface Science*, vol. 243, no. 1–4, pp. 245–250, 2005.

[22] P. P. Yang, S. L. Gai, Y. C. Liu, W. X. Wang, C. X. Li, and J. Lin, "Uniform hollow Lu_2O_3:Ln (Ln = Eu^{3+}/Tb^{3+}) spheres: facile synthesis and luminescent properties," *Inorganic Chemistry*, vol. 50, no. 6, pp. 2182–2190, 2011.

[23] N. Niu, P. P. Yang, F. He et al., "Tunable multicolor and bright white emission of one-dimensional $NaLuF_4$:Yb^{3+}, Ln^{3+}

(Ln = Er, Tm, Ho, Er/Tm, Tm/Ho) microstructures," *Journal of Materials Chemistry*, vol. 22, no. 21, pp. 10889–10899, 2012.

[24] E. W. Barrera, M. C. Pujol, F. Díaz et al., "Emission properties of hydrothermal Yb^{3+}, Er^{3+} and Yb^{3+}, Tm^{3+}-codoped Lu_2O_3 nanorods: upconversion, cathodoluminescence and assessment of waveguide behavior," *Nanotechnology*, vol. 22, no. 7, Article ID 075205, 2011.

[25] Y. P. Li, J. H. Zhang, Y. S. Luo, X. Zhang, Z. D. Hao, and X. J. Wang, "Color control and white light generation of upconversion luminescence by operating dopant concentrations and pump densities in Yb^{3+}, Er^{3+} and Tm^{3+} tri-doped Lu_2O_3 nanocrystals," *Journal of Materials Chemistry*, vol. 21, no. 9, pp. 2895–2900, 2011.

[26] X. Wang and Y. D. Li, "Rare-earth-compound nanowires, nanotubes, and fullerene-like nanoparticles: synthesis, characterization, and properties," *Chemistry*, vol. 9, no. 22, pp. 5627–5635, 2003.